International Journal of Heat and Mass Transfer 51 (2008) 6090–6101

Contents lists available at ScienceDirect

International Journal of Heat and Mass Transfer

journal homepage: www.elsevier.com/locate/ijhmt

Convective condensation of vapor in the presence of a non-condensable gas of high concentration in laminar flow in a vertical pipe

V. Dharma Rao [a,*], V. Murali Krishna [b], K.V. Sharma [c], P.V.J. Mohana Rao [d]

[a] Department of Chemical Engineering, College of Engineering, Andhra University, Visakhapatnam 530 003, India
[b] Department of Mechanical Engineering, GVP College of Engineering, Visakhapatnam 530 041, India
[c] Department of Mechanical Engineering, JNTU, Hyderabad 500 085, India
[d] Department of Marine Engineering, College of Engineering, Andhra University, Visakhapatnam 530 003, India

ARTICLE INFO

Article history:
Received 3 September 2007
Received in revised form 29 February 2008
Available online 2 June 2008

Keywords:
High concentration
Non-condensable gas
Condensation
Vertical pipe
Laminar forced convection
Two-phase flow

ABSTRACT

The problem of laminar film condensation of vapor in the presence of high concentration non-condensable gas such as humid air flowing in a vertical pipe under laminar forced convection conditions is formulated theoretically. The vapor condensing at dew point temperature releases both sensible and latent heats and diffuses on to the surface of the pipe through a non-condensable gas film. Thus it is treated as combined heat and mass transfer problem governed by mass, momentum and energy balance equations for the vapor–gas mixture and diffusion equation for the vapor species. The flow of the falling condensate film is governed by the momentum and energy balance equations. The temperature at the gas-to-liquid interface, at which the condensation takes place, is estimated with the help of the heat balance and mass balance equations at the interface. The local and average values of the condensation Nusselt number, condensate Reynolds number, gas–liquid interface temperature and pressure drop are estimated from the numerical results for different values of the system parameters at inlet, such as relative humidity, temperature of vapor–gas mixture, gas phase Reynolds number and total pressure. The gas phase convection Nusselt and Sherwood numbers are also computed from numerical results. The predictions of the present study are compared with the experimental data available in literature, and the agreement is found to be reasonably good. An implicit pressure correction method developed by the authors is used in solving the momentum balance equation for the gas phase.

1. Introduction

Condensation of water vapor from the vapor–gas mixture with a high-percentage of non-condensable gas is of great importance in a number of engineering applications such as air cleaning and conditioning systems, humidity control systems, atmospheric condensers, refrigeration engineering, heat exchangers with narrow channels, condensation of waste vapors in heat power installations, etc. The vapor–gas mixture flows down in a vertical pipe. The temperature of pipe wall is less than the dew point temperature of the mixture. Vapor condenses on the inner wall of the pipe and flows down as a film. The vapor diffuses through the convection boundary layer and condenses on the pipe wall. Hence the total heat flux received at the wall is the sum of sensible and latent heats due to convection and condensation respectively. Thus the heat and mass transfer processes are interrelated during the condensation of vapor presenting a complex phenomenon, which needs a combined solution of continuity, momentum and energy balances, and the diffusion equation. If the wall of the pipe is below the freezing temperature of the condensate, then the condensate on the wall solidifies. In the present analysis the wall of the pipe is maintained above the freezing temperature of the liquid, thus precluding the possibility for freezing of condensate.

The annular filmwise condensation of pure vapor inside a vertical tube was studied extensively [1–7]. Carpenter and Colburn [1] were the first to treat analytically the convective condensation of vapor inside tubes, when the vapor in turbulent flow in the tube. They studied the effect of vapor shear on the flow of the condensate film. Shekriladze and Mestvirishvili [2] tackled theoretically the problem of film condensation of moving vapor in a descending flow inside a vertical tube by using von Karman integral relation to determine the inter-phase friction and pressure gradient. Lucas and Moser [3] studied the laminar film condensation of pure vapors in tubes. They concluded that the effect of the heat transfer to the surroundings and the orientation of the tube can be quite considerable. Dobran and Thorsen [4] conducted an analytical study for laminar filmwise condensation of a saturated vapor in

* Corresponding author. Tel.: +91 891 254 0391; fax: +91 891 275 5324.
E-mail addresses: v.dharmarao@yahoo.com (V. Dharma Rao), mk_vemula@rediffmail.com (V. Murali Krishna), kvsharmajntu@yahoo.com (K.V. Sharma), pvjmr@hotmail.com (P.V.J. Mohana Rao).

0017-9310/$ - see front matter © 2008 Elsevier Ltd. All rights reserved.
doi:10.1016/j.ijheatmasstransfer.2008.03.027

Nomenclature

Ar_0	Archimedes number ($gD^3/\nu_{g,0}^2$)
C_p	specific heat at constant pressure (J kg^{-1} K^{-1})
$C_{p,g}^+$	normalized gas specific heat at constant pressure ($C_{p,g}/C_{p,g,0}$)
D	diameter of the pipe (m)
d	moisture content (gm water vapor per kg dry air)
d_e	equivalent diameter (m)
D_{va}	mass diffusion coefficient of water vapor in air (m^2 s^{-1})
D_{va}^+	normalized mass diffusion coefficient ($D_{va}/D_{va,0}$)
F	factor, see Eq. (22)
g	gravitational acceleration (m s^{-2})
h_l	local condensation heat transfer coefficient (W m^{-2} $^{-1}$)
h_g	local convection heat transfer coefficient (W m^{-2} K^{-1})
h_D	local diffusion mass transfer coefficient (m^2 s^{-1})
k	thermal conductivity (W m^{-1} K^{-1})
k^+	gas-to-liquid thermal conductivity ratio (k_g/k_l)
k_g^+	normalized gas thermal conductivity ($k_g/k_{g,0}$)
L	length of the pipe (m)
L^+	Normalized length of pipe ($L/DRe_{g,0}$)
$\dot{m}$	condensate mass flux (kg m^{-1} s^{-1})
n	number of moles (kg mol)
Nu_l	condensation Nusselt number ($h_l D/k_l$)
Nu_g	convection Nusselt number ($h_g D/k_g$)
P	total pressure (bar)
Pr	Prandtl number (μC_p/k)
p	partial pressure (bar)
$Re_{g,0}$	gas phase Reynolds number at inlet ($\rho_{g,0}u_0D/\mu_{g,0}$)
Re_l	condensate Reynolds number ($4\dot{m}_l/\mu_l$)
R_H	relative humidity (p_v/p_v^*) (%)
R	inner radius of the pipe ($D/2$) (m)
r	radial coordinate
r^+	non-dimensional radial coordinate (r/D)
q	heat flux (W m^{-2})
S	sub-cooling parameter ($C_{p,l}(T_0 - T_w)/\lambda_0$)
Sc	Schmidt number ($\mu_g/\rho_g D_{va}$)
Sh	Sherwood number ($h_D D/D_{va}$)
T	temperature of gas–vapor mixture (K)
T^+	normalized temperature ($T - T_w$)/($T_0 - T_w$)
u	component of air velocity in z-direction (m s^{-1})
u^+	normalized u-velocity (u/u_0)
V	total volume of gas–vapor mixture (m^3)
v	component of air velocity in radial direction (m s^{-1})
v^+	normalized v-velocity ($v\,Re_g/u_0$)
y	coordinate (see Fig. 1)
Y_v	mole fraction of vapor (p_v/P)
Y_a	mole fraction of air ($1 - Y_v$)
z	down stream distance (m)
z^+	normalized distance in z-direction (z/DRe_g)

Greek symbols

β	temperature ratio parameter (($T_0 - T_w$)/T_w)
δ_l	thickness of the condensate film (m)
δ_l^+	normalized condensate film thickness (δ/D)
ΔP	pressure drop of vapor–air mixture (k Pa)
λ	latent heat of condensation (J kg^{-1})
λ^+	normalized latent heat of condensation (λ/λ_0)
μ	dynamic viscosity (kg m^{-1} s^{-1})
μ^+	gas-to-liquid viscosity ratio (μ_g/μ_l)
μ_g^+	normalized gas viscosity ($\mu_g/\mu_{g,0}$)
ν	kinematic viscosity (μ/ρ) (m^2 s^{-1})
ρ	density (kg m^{-3})
ρ_g^+	normalized gas density ($\rho_g/\ \rho_{g,0}$)
ρ_v^+	normalized vapor density ($\rho_v/\rho_{v,0}$)
$\rho_{g,v}^+$	density ratio parameter ($\rho_g/\rho_{v,0}$)
τ	shear stress (N m^{-2})

Subscripts

0	inlet
a	air species
av	average
d	dew point
e	exit i.e., at $z = L$
g	gas phase, i.e., air–water vapor mixture
g,i	gas at gas-to-liquid interface at $r = (R - \delta_l)$ (or) $r^+ = (0.5 - \delta_l^+)$
i	gas-to-liquid interface i.e., at $r = (R - \delta_l)$ (or) $r^+ = (0.5 - \delta_l^+)$
l	liquid (condensate)
l,i	liquid at gas-to-liquid interface at $r = (R - \delta_l)$ (or) $r^+ = (0.5 - \delta_l^+)$
tot	total
v	water vapor
w	wall

forced flow in a vertical tube. They found that the process of condensation is governed by ratio of vapor Froude number to Reynolds number, vapor to liquid viscosity ratio, liquid Prandtl number and subcooling number. Seban and Hodgson [5] investigated the problem of laminar film condensation for the case of upward vapor flow in the inside of a vertical tube for different inlet conditions, tube sizes and pressures. Blangetti et al. [6] measured local heat transfer coefficients for pure vapor condensation during downward flow of vapor inside a vertical tube for moderate and high liquid Prandtl numbers. Kim and No [7] performed an experimental study to investigate the high pressure steam condensation heat transfer in a vertical condenser tube. They measured the film condensation heat transfer coefficients and two-phase pressure drops.

Studies on the in-tube condensation of vapor in the presence of a non-condensable gas can be divided into two categories, as those involving low and high concentrations of the non-condensable gas, respectively. Traces of non-condensable gases may enter into the condenser either as gases dissolved in the boiler feed water or due to leakage in the condenser. The effect of the presence of these gases on the process of condensation of vapor inside vertical tubes and channels was studied in literature [8–23]. It is found that the existence of low percentage of non-condensable gas in vapors greatly reduces the heat transfer and the condensation rates. Borishansky et al. [8] conducted experiments for condensation inside tubes, with and without non-condensable gases. They developed an expression relating the reduction in the overall pure steam heat transfer coefficient to the inlet mole fraction of the non-condensable nitrogen. Wang and Tu [9] developed a theoretical model to include the effect of small amounts of non-condensable gas on laminar film-wise condensation of a vapor-gas mixture in turbulent flow through a vertical tube based on the analogy between condensation and convective transport with boundary suction. They found that the reductions in heat transfer due to the non-condensable gas are found to be more significant at low pressures and at low Reynolds numbers of the mixtures. Kageyama et al. [10] developed a diffusion boundary layer model for condensation of steam in a vertical tube in the presence of a non-condensable gas using the concept of effective condensation thermal conductivity. Peterson et al. [11] extended the diffusion boundary layer model

of Kageyama et al. [10] for the cases of condensation of vapor in turbulent flow in a vertical tube and that over a vertical surface. The vapor contains a non-condensable gas in low concentration. Siddique et al. [12] conducted an experimental investigation to determine the local condensation heat transfer coefficients of steam–air and steam–helium mixtures flowing downward inside a vertical tube. Siddique et al. [13] also developed an analytical model to determine local condensation heat transfer coefficients for the vapor–gas mixture flowing down inside a vertical tube using the analogy between heat and mass transfer. They included the effects of developing flow, condensate film roughness, and property variation in the gas phase in their model. The model developed by Siddique et al. [13] is extended by Hasanein et al. [14] to the in-tube steam condensation under forced convection conditions in the presence of more than one non-condensable gas such as air/helium mixtures. According to them the thermal resistance offered by the condensate film can be significant, when the Reynolds number of the gas mixture is high (>6000) and the mass fraction of the non-condensable gases in the mixture is low (<0.2). Munoz-Cobo et al. [15] developed a model to predict the condensate film thickness and local heat transfer coefficient for laminar film-wise condensation of vapor in turbulent flow in a vertical tube in the presence of a non-condensable gas. They found that at high Reynolds numbers the heat transfer coefficients strongly depend on the interfacial shear stresses. Studies on the condensation of vapor in the presence of non-condensable gas in vertical tube are also available in literature [16–23]. Dehbi and Guentay [16] included the effect of interfacial shear stress on condensation, and they used heat and mass transfer analogy to obtain condensation rates. They investigated the effect of the system parameters such as the inlet gas fraction, the mixture inlet flow rate and the total pressure on the performance of the condenser. Khun et al. [17] measured experimentally the local heat fluxes for the condensation of pure steam, steam–air mixtures and steam–helium mixtures. They also developed correlations for local heat transfer coefficient using degradation factor method, diffusion layer theory, and mass transfer conductance model. Herranz et al. [18] developed a theoretical model based on heat and mass transfer analogy and by considering the effect of the presence of a non-condensable gas by diffusion in a boundary layer. The model also included the effects of suction, flow development, film waviness, and droplet entrainment. No and Park [19] developed a theoretical non-iterative condensation model using heat and mass transfer analogy considering the effects of high mass transfer rates, entrance and interfacial waviness on condensation. Maheshwari et al. [20] incorporated the effects of film waviness, suction, developing flow and property variation of the gas phase for the case of turbulent flow of vapor–gas mixture inside a vertical tube. Oh and Revankar [21] found from the experiments that the condensation heat transfer coefficient decreases with the presence of a non-condensable gas. They also developed a theoretical model for the annular filmwise condensation with non-condensable gas using heat and mass transfer analogy. Siow et al. [22] obtained numerical results for the case of laminar film condensation from steam–air mixtures in a vertical parallel plate channel using a fully-coupled implicit numerical approach. They estimated local and average condensation Nusselt numbers, condensate film thickness and pressure gradient from numerical results for steam–air mixtures over wide ranges of four independent system parameters, such as non-condensable gas concentration, gas phase Reynolds number, pressure gradient, and the difference between the inlet and wall temperatures. Groff et al. [23] developed a complete two-phase model for film condensation from turbulent downward flow of vapor–gas mixtures in a vertical tube using finite volume method. The model solves the complete parabolic governing equations in both gas and liquid phases including the effect of turbulence in each phase, without using additional correlation equations for interfacial heat and mass transfer. However all of the above studies are concerned with the presence of non-condensable gas in low concentrations only.

The problem in the present investigation relates to the case of vapor condensation containing high percentage of non-condensable gas, such as air. Lebedev et al. [24] performed an experimental study of combined heat and mass transfer in vapor condensation from humid air. They observed an increase in condensation heat transfer with an increase in the relative humidity and velocity of the air. Smol'skii et al. [25] and Novikov and Shcherbakov [26] conducted experiments to find heat and mass transfer during condensation of water vapor from humid air in narrow channels. Smol'skii et al. [27] performed experiments and found that, the pressure drop during condensation of vapor from humid air is much higher than that in a one-phase stream. Desrayaud and Lauriat [28] presented analytical results for heat and mass transfer during condensation of vapor from humid air in a vertical parallel plate channel under natural convection conditions and established correlations for latent and sensible Nusselt numbers using Reynolds analogy. Pele et al. [29] studied the effect of the flow rate of saturated humid air on laminar film-wise condensation of vapor flowing inside a cooled vertical pipe under turbulent forced convection conditions. They found that the local condensation heat transfer coefficient decreases along the length of the pipe. Terekhov et al. [30] tackled the problem of condensation of humid air by solving integral boundary layer equations for energy and diffusion and using analogy between heat and mass transfer processes. Terekhov and Patrikeev [31] obtained experimental and numerical results for condensation of vapor from humid air in a channel at elevated pressures in forced convection. They studied the effect of temperature and concentration boundary conditions on the heat and mass transfer coefficients for different inlet conditions. Volchkov et al. [32] obtained numerical solution of the system of differential energy, diffusion, and boundary layer flow equations for the laminar and turbulent flows of humid air with surface steam condensation. Terekhov and Patrikeev [31] and Volchkov et al. [32] ignored the thermal resistance offered by the condensate film formed on the duct wall in view of very low condensation rates. Dharma Rao et al. [33] tackled theoretically the problem of condensation of water vapor from humid air in turbulent flow in a vertical duct. They obtained local and average values of the condensation Nusselt number, condensate Reynolds number, gas–liquid interface temperature and pressure drop from the numerical results for different values of the system parameters at inlet, such as relative humidity, temperature of air, gas phase Reynolds number and total pressure.

The problem of condensation of vapor in the presence of high concentration non-condensable gas in laminar flow through a vertical pipe is tackled theoretically. The condensate film on the wall of the pipe is assumed to be a thin film in laminar flow. The condensation rates are obtained by a conjugate analysis of the problem of forced convection of the vapor–gas mixture in the pipe with the Nusselt's analysis of condensation for the condensate film. The equations of continuity, momentum, energy and diffusion for the vapor–gas mixture are solved along with momentum and energy balance equations for the condensate film and the mass and heat balances involving condensation at the free surface of the condensate film.

2. Physical model and formulation

Steady, laminar, filmwise condensation of vapor from a mixture of a vapor and a non-condensable gas in high concentration flowing in a vertical tube with down flow is considered. The inner diameter of the tube is D and length of the tube is L. The flow of the vapor–gas mixture is laminar. The physical model under

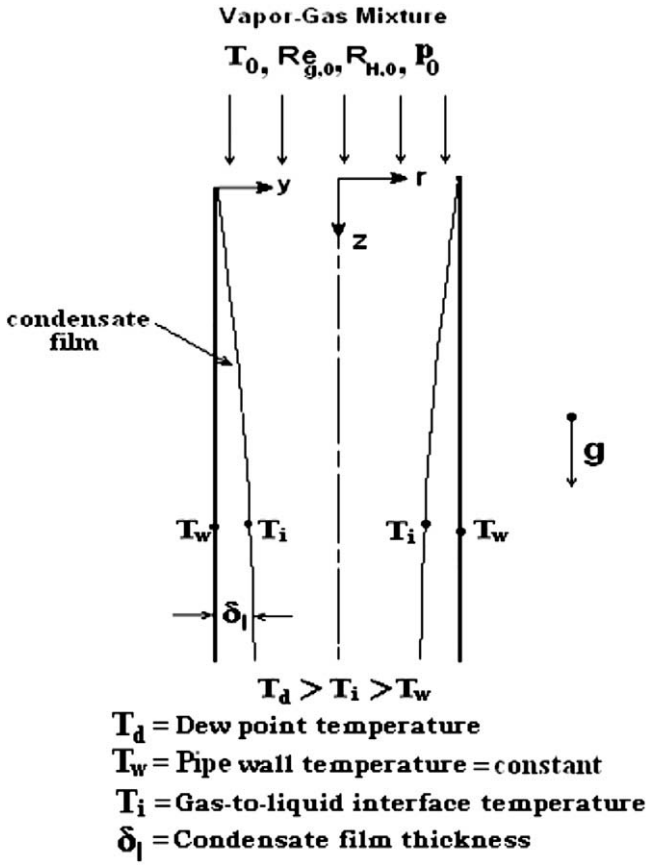

Fig. 1. Physical model and configuration.

consideration is illustrated schematically in Fig. 1. The flow is two-dimensional and symmetrical about the center line of the pipe. The u and v are the velocity components in z-direction (flow direction) and radial direction respectively. The water vapor–gas mixture enters at inlet of the pipe with a Reynolds number $Re_{g,0}$, temperature T_0, total pressure P_0 and relative humidity $R_{H,0}$. The tube surface is maintained at a constant temperature, T_w, and $T_w < T_0$. The partial pressure of water vapor at inlet $p_{v,0}$ can be obtained as $p_{v,0} = (R_{H,0})\left(p^*_{v,0}\right)$, where $p^*_{v,0}$ is the saturation vapor pressure of water at temperature T_0. $p^*_{v,0}$ is to be obtained from the vapor pressure data of water. The vapor pressure data are correlated in the form of an expression as shown below for the purpose of ready computation. The correlation equation given below is obtained with the help of the saturation vapor pressure data of water prepared by Schmidt and Grigull [34].

$$p^*_v = \exp\left(18.79 - 0.0075T - \frac{5965.6}{T}\right) \tag{1}$$

T and p^*_v are temperature in Kelvin and saturation vapor pressure in bar respectively. Eq. (1) predicts the saturation vapor pressures with a maximum deviation of ±0.4%with the data of [34] over the temperature range from 5 °C to 40 °C, which is the operating range of temperature in our numerical results.

The density of water vapor, ρ_v and density of air ρ_a, respectively are given by

$$\rho_v = \frac{p_v}{R_v T}, \quad \rho_a = \frac{(P - p_v)}{R_a T} \tag{2}$$

The density of the vapor–air mixture, ρ_g is given by

$$\rho_g = \rho_v + \rho_a \tag{3}$$

where $R_v = 462 \times 10^{-5}$ bar m^3/kg water–K and $R_a = 287 \times 10^{-5}$ bar m^3/kg air–K. At the inlet, i.e., at $z = 0$, the total pressure and temperature of the vapor–air mixture, P_0 and T_0, and the partial pressure of water vapor, $p_{v,0}$ are prescribed. The partial pressure of air species at inlet is equal to $(P_0 - p_{v,0})$. The densities of the vapor and air are calculated using Eq. (2). The density of the vapor–air mixture at inlet, $\rho_{g,0}$ is calculated using Eq. (3). Since air does not condense at the system conditions, its density ρ_a remains constant.

Water vapor condenses if the vapor–air mixture is cooled below its dew point temperature, T_d. The dew point temperature, T_d, at any distance from inlet, z, in the pipe corresponds to the partial pressure of the water vapor corresponding to the temperature and total pressure at the position, z. The dew point temperature can be calculated from the vapor pressure data of water vapor and these data are correlated in the form of an expression as shown below.

$$T_d = 66.622(-B + \sqrt{B^2 - 44.772}) \tag{4}$$

where $B = 18.79 - \log_e(p_v)$, and T_d and p_v are dew point temperature in Kelvin and vapor pressure in bar, respectively. The vapor condensing at the dew point temperature diffuses towards the tube wall through the air film. As the mixture starts flowing down the tube, the vapor condenses from the vapor–air mixture to form a condensate layer of thickness δ_l on the tube surface. The flow of the condensate is caused by gravity and also by the shear force acting on the film surface by the flowing gas. Since the rate of condensation is expected to be low, the condensate film is assumed to be thin. The temperature on the free surface of the condensate is T_i which is less than dew point temperature, T_d. T_i is an unknown temperature, which has to be evaluated by a trial-and-error procedure. In formulating the problem of condensation of vapor from the flowing air–vapor mixture, it is assumed that the gas-to-liquid interface is smooth and the vapor–air mixture is treated as an ideal gas mixture. The total pressure, P, is assumed to be constant across the tube i.e., $\partial P/\partial r = 0$, however, P varies in the z-direction due to friction loss, momentum change and hydrostatic pressure loss. All the properties in the governing equations of gas phase and liquid phase are considered to be functions of temperature and pressure. The governing equations for the gas phase and the condensate film are given below.

2.1. Gas phase

The mass, momentum and energy balance equations for the gas phase and the diffusion equation for the vapor species in cylindrical coordinate system are written as follows. The density of the gas phase, ρ_g is assumed to be a function of z alone.

Mass balance

$$\frac{\partial u}{\partial z} + \frac{1}{r}\frac{\partial}{\partial r}(vr) + \frac{u}{\rho_g}\frac{\partial \rho_g}{\partial z} = 0 \tag{5}$$

Momentum balance

$$u\frac{\partial u}{\partial z} + v\frac{\partial u}{\partial r} = -\frac{1}{\rho_g}\frac{dp}{dz} + \nu_g\left(\frac{\partial^2 u}{\partial r^2} + \frac{1}{r}\frac{\partial u}{\partial r}\right) + g \tag{6}$$

Energy balance

$$u\frac{\partial T}{\partial z} + v\frac{\partial T}{\partial r} = \left(\frac{\nu_g}{Pr_g}\right)\left(\frac{\partial^2 T}{\partial r^2} + \frac{1}{r}\frac{\partial T}{\partial r}\right) \tag{7}$$

Diffusion

$$u\frac{\partial \rho_v}{\partial z} + v\frac{\partial \rho_v}{\partial r} - \rho_v\left(\frac{v}{r} + \frac{u}{\rho_g}\frac{\partial \rho_g}{\partial z}\right) = \left(\frac{\nu_g}{Sc_g}\right)\left(\frac{\partial^2 \rho_v}{\partial r^2} + \frac{1}{r}\frac{\partial \rho_v}{\partial r}\right) \tag{8}$$

2.2. Liquid phase

As the thickness of the condensate film is by far less compared to the radius of the pipe, a simplifying assumption is made by neglecting the effect of the radius of curvature in the evaluation of the thickness of the condensate film. Thus the momentum and energy balance equations for the liquid film are simplified to the form as shown below.

Momentum balance

$$\frac{\partial^2 u}{\partial y^2} + \frac{g(\rho_l - \rho_v)}{\mu_l} = 0 \tag{9}$$

where y is the distance measured from the wall of the pipe, and $y = (R - r)$. The inertial force term in the above equation is neglected due to low rate of condensation.*Energy balance*

$$\frac{\partial^2 T}{\partial y^2} = 0 \tag{10}$$

The advection terms are neglected in the above equation following Nusselt.

2.3. Boundary conditions

The governing equations for the gas phase ($0 \leqslant r \leqslant (R - \delta_l)$) and condensate film ($(R - \delta_l) \leqslant r \leqslant R$) i.e., Eqs. (5)–(10) are coupled and solved using the following boundary conditions.

For $z = 0$, i.e., at the inlet of pipe

$$u = u_0, \quad v = 0, T = T_0, \quad \rho_g = \rho_{g,0}, \quad \rho_v = \rho_{v,0} \text{ for } 0 \leqslant r \leqslant R \tag{11}$$

$$\text{For } z > 0 : \text{At the center line i.e., } r = 0 : \frac{\partial u}{\partial r} = 0, \quad v = 0, \quad \frac{\partial T}{\partial r} = 0,$$

$$\frac{\partial \rho_v}{\partial r} = 0 \tag{12}$$

$$\text{At the wall i.e., } r = R : u = 0, \quad v = 0, \quad T = T_w = \text{constant} \tag{13}$$

$$\text{At gas-to-liquid interface i.e., at } r = R - \delta_l, \quad u = u_i \text{ and } T = T_i \tag{14}$$

where δ_l is the thickness of the condensate film, R is the inner radius of pipe and the subscript 'i' refers to the gas-to-liquid interface.

2.4. Gas-to-liquid interface balances

The balances at the gas-to-liquid interface are described as follows:

Velocity

$$u_i = u_{l,i} = u_{g,i} \tag{15}$$

Temperature

$$T_i = T_{l,i} = T_{g,i} \tag{16}$$

Shear stress

The shear balance between the flowing gas stream and the condensate film at the interface is given by

$$\tau_{l,i} = \tau_{g,i} \tag{17}$$

where $\tau_{l,i} = -\mu_l \frac{\partial u}{\partial r}\big|_{l,i}$ and $\tau_{g,i} = -\mu_g \frac{\partial u}{\partial r}\big|_{g,i}$

Mass balance

The mass balance at the interface i.e., at r=(R-δ_l) is given by the following equation:

$$\frac{d\dot{m}_l}{dz} = \frac{D_{va}}{1 - (C_{v,i}/\overline{C}_i)} \left(\frac{-\partial \rho_v}{\partial r}\bigg|_i \right) \tag{18}$$

where

$$\frac{C_{v,i}}{\overline{C}_i} = \frac{\rho_{v,i} R_v T_i}{18P}.$$

Heat balance

Heat transfer from the vapor–gas mixture to the liquid film at the interface comprises two components namely the sensible heat by convection and the latent heat released by the condensing vapor. Then the heat flux at gas-to-liquid interface can be written as follows:

$$q_{l,i} = q_{g,i} + \lambda_i \frac{d\dot{m}_l}{dz} \tag{19}$$

where $q_{l,i}$ = total heat flux received by the condensate film; $q_{g,i}$ = heat flux transferred by convection from the gas; λ_i = latent heat of condensation of vapor at temperature, T_i.

The latent heat at any temperature is computed from the following equation:

$$\lambda(\text{J kg}^{-1}) = 2.7554 \times 10^6 - 3.464\text{T}^2 \tag{20}$$

Eq. (20) is deduced from Clausius-Clapeyron equation given by Wark and Richards [35] with the aid of the expression for p_v^* given by Eq. (1).

2.5. Condensate film thickness, δ_l

The following velocity profile in the condensate film is obtained by integrating Eq. (9) using the boundary conditions given by Eqs. (13) and (14)

$$\frac{u}{u_i} = \frac{y}{\delta_l}\left[1 + F\left(1 - \frac{y}{\delta_l}\right)\right] \tag{21}$$

where the factor F is given by the following equation:

$$F = \frac{g(\rho_l - \rho_v)\delta_l^2}{2\mu_l u_i} \tag{22}$$

The condensation rate per unit perimeter of the pipe, $\dot{m}_l$ can be obtained from the following equation:

$$\dot{m}_l = \rho_l \int_{(R-\delta_l)}^{R} u dr \tag{23}$$

The integral in the above equation is evaluated using the velocity profile, i.e., Eq. (21), and the following equation is obtained for condensate mass flow rate per unit perimeter of the film

$$\dot{m}_l = \frac{\rho_l u_i \delta_l}{2}\left(1 + \frac{F}{3}\right) \tag{24}$$

From the Eqs. (17) and (21) the velocity at the gas-to-liquid interface i.e., at $r = (R - \delta_l)$ is given by the following expression:

$$u_i = \frac{\delta_l}{\mu_l(1 - F)} \mu_g \frac{\partial u}{\partial r}\bigg|_{g,i} \tag{25}$$

The values of the derivative $\partial u/\partial r|_g$ at r = $(R - \delta_l)$, appearing in Eq. (25), is to be obtained from the numerical results for the gas phase i.e., for the vapor-gas mixture flowing in a tube. From the Eqs. (24) and (25), an equation for condensate film thickness, δ_l is obtained as shown below.

$$\delta_l = \left[\frac{2\nu_l \dot{m}_l}{\mu_g} \frac{1}{(\partial u/\partial r)|_{g,i}} \frac{(1 - F)}{(1 + F/3)}\right]^{1/2} \tag{26}$$

2.6. Gas-to-liquid interface temperature, T_i

Integration of Eq. (10) using the boundary conditions given in Eqs. (13) and (14) yields the following temperature profile for the condensate liquid film

$$\frac{T - T_w}{T_i - T_w} = \frac{y}{\delta_l} \tag{27}$$

Making use of the above temperature profile, the heat flux $q_{l,i}$ is given by

$$q_{l,i} = k_l \frac{T_i - T_w}{\delta_l} \tag{28}$$

Thus from Eqs. (19) and (28), the temperature at gas-to-liquid interface, T_i, is given by the following equation:

$$T_i = T_w + \delta_l \left[-\frac{k_g}{k_l} \frac{\partial T}{\partial r}\bigg|_{g,i} + \frac{\lambda_i}{k_l} \frac{d\dot{m}_l}{dz} \right] \tag{29}$$

Eq. (29) is in implicit form to estimate T_i, since the terms δ_l, $(d\dot{m}_l/dz)$, $\partial T/\partial r|_{g,i}$ on the RHS are also function of T_i.

2.7. Heat and mass transfer coefficients

The local condensation heat transfer coefficient, h_l, which includes both convection and condensation heat transfer rates, is defined as given below

$$-k_l \frac{\partial T}{\partial r}\bigg|_{l,i} = h_l (T_{av} - T_w) \tag{30}$$

where T_{av} is the local bulk temperature of the gas–vapor mixture in the pipe. The bulk temperature, T_{av} is determined as an integrated average of the local fluid temperature in radial direction at a specified z. The local convection heat transfer coefficient for the gas phase, h_g, is defined by the following equation:

$$-k_g \frac{\partial T}{\partial r}\bigg|_{g,i} = h_g (T_{av} - T_w) \tag{31}$$

The local diffusion mass transfer coefficient (h_D) is defined by the following equation:

$$-D_{va} \frac{\partial \rho_v}{\partial r}\bigg|_{i} = h_D \rho_{v,av} \tag{32}$$

where $\rho_{v,av}$ is the local mean density of the vapor across the pipe in the gas phase.

2.8. Normalized equations for gas and liquid phases

The constitutive equations are put in the normalized form making use of the following dimensionless variables and parameters

$$u^+ = u/u_0; \quad v^+ = vRe_g/u_0; \quad T^+ = (T - T_w)/(T_0 - T_w); \quad \rho_g^+ = \rho_g/\rho_{g,0};$$
$$\rho_v^+ = \rho_v/\rho_{v,0}; \quad z^+ = z/DRe_g$$
$$r^+ = r/D; \quad \delta_l^+ = \delta_l/D; \quad \rho_{g,v}^+ = \rho_g/\rho_{v,0}; \quad k^+ = k_g/k_l; \quad \mu^+ = \mu_g/\mu_l$$
$$v^+ = \nu_g/\nu_l; \quad \lambda_i^+ = \lambda_i/\lambda_0$$
$$Re_g = u_0 D/\nu_g; \quad Sc_g = \nu_g/D_{va}; \quad Re_l = 4\dot{m}_l/\mu_l; \quad P^+ = (P - P_0)/\rho_{g,0} u_0^2;$$
$$Ar = gD^3/\nu_g^2 \tag{33}$$

2.8.1. Normalized gas phase equations

The equations of mass, momentum, energy and species for gas phase i.e., Eqs. (5)–(8) are written in normalized form as follows:

Continuity equation

$$\frac{\partial u^+}{\partial z^+} + \frac{1}{r^+} \frac{\partial (v^+ r^+)}{\partial r^+} + \frac{u^+}{\rho_g^+} \frac{\partial \rho_g^+}{\partial z^+} = 0 \tag{34}$$

Momentum equation

$$u^+ \frac{\partial u^+}{\partial z^+} + v^+ \frac{\partial u^+}{\partial r^+} = -\frac{1}{\rho_g^+} \frac{\partial P^+}{\partial z^+} + \left(\frac{\partial^2 u^+}{\partial r^{+2}} + \frac{1}{r^+} \frac{\partial u^+}{\partial r^+} \right) + \frac{Ar}{Re_g} \tag{35}$$

Energy equation

$$u^+ \frac{\partial T^+}{\partial z^+} + v^+ \frac{\partial T^+}{\partial r^+} = \frac{1}{Pr_g} \left(\frac{\partial^2 T^+}{\partial r^{+2}} + \frac{1}{r^+} \frac{\partial T^+}{\partial r^+} \right) \tag{36}$$

Diffusion equation

$$u^+ \frac{\partial \rho_v^+}{\partial z^+} + v^+ \frac{\partial \rho_v^+}{\partial r^+} - \rho_v^+ \left(\frac{v^+}{r^+} + \frac{u^+}{\rho_g^+} \frac{\partial \rho_g^+}{\partial z^+} \right) = \frac{1}{Sc_g} \left(\frac{\partial^2 \rho_v^+}{\partial r^{+2}} + \frac{1}{r^+} \frac{\partial \rho_v^+}{\partial r^+} \right) \tag{37}$$

where

$$Re_g = Re_{g,0} \frac{\rho_g^+}{\mu_g^+}, \quad Pr_g = Pr_{g,0} \frac{\mu_g^+ C_{pg}^+}{k_g^+} Sc_g = Sc_{g,0} \frac{\mu_g^+}{\rho_g^+ D_{va}^+} \text{ and}$$
$$Ar = Ar_0 \left(\frac{\nu_{g,0}}{\nu_g} \right)^2 \tag{38}$$

2.8.2. Normalized boundary conditions

The boundary conditions in normalized form are as follows:

At the inlet i.e. at $z^+ = 0$

$$u^+ = 1, \quad T^+ = 1, \quad \rho_g^+ = 1, \quad \rho_v^+ = 1 \text{ for } 0 \leqslant r^+ \leqslant 0.5 \tag{39}$$

For $z^+ > 0$

$$\frac{\partial u^+}{\partial r^+} = 0, \quad \frac{\partial T^+}{\partial r^+} = 0, \quad v^+ = 0, \quad \frac{\partial \rho_v^+}{\partial r^+} = 0 \quad \text{at } r^+ = 0 \tag{40}$$
$$u^+ = 0, \quad T^+ = 0, \quad \rho_v^+ = 0 \text{ at } y^+ = 0.5 \tag{41}$$
$$u^+ = u_i^+, \quad T^+ = T_i^+, \quad \rho_v^+ = \rho_{v,i}^+ \text{ at } r^+ = (0.5 - \delta_l^+) \tag{42}$$

2.8.3. Normalized equations for the gas-to-liquid interface

The normalized form of mass balance equation at the interface i.e., Eq. (18) is written as follows:

$$\frac{dRe_l}{dz^+} = \frac{4\mu^+}{Sc_g} \frac{Re_g}{\rho_{g,v}^+} \frac{(-\partial \rho_v^+/\partial r^+)|_i}{1 - (C_{v,i}/\overline{C}_i)} \tag{43}$$

where

$$\frac{C_{v,i}}{\overline{C}_i} = \left(\frac{p_{v,0}}{T_0} \right) \left(\frac{\beta T_i^+ + 1}{P} \right) \rho_{v,i}^+ \tag{44}$$

The dimensionless condensate film thickness (δ_l^+), which is obtained from Eq. (26), is given by the following equation:

$$\delta_l^+ = \left(\frac{Re_l}{2\nu^+ \mu^+ Re_g} \frac{1}{\partial u^+/\partial r^+|_{g,i}} \frac{(1-F)}{(1+F/3)} \right)^{1/2} \tag{45}$$

It is assumed that the value of F is by far less than unity. So the δ_l^+ can be computed from the following equation:

$$\delta_l^+ = \left(\frac{Re_l}{2\nu^+ \mu^+ Re_g} \frac{1}{\partial u^+/\partial r^+|_{g,i}} \right)^{1/2} \tag{46}$$

The maximum value of F is found to be 0.049 from numerical results for the system parameters considered in the present analysis. Thus, the assumption made is justified. From the Eq. (29), the normalized temperature at gas-to-liquid interface, T_i^+ is given by the following equation:

$$T_i^+ = \delta_l^+ \left[-k^+ \frac{\partial T^+}{\partial r^+}\bigg|_{g,i} + \frac{Pr_1}{4S} \frac{\lambda_i^+}{Re_g} \frac{dRe_1}{dz^+} \right] \tag{47}$$

2.9. Nusselt and Sherwood numbers

The local condensation Nusselt number, $Nu_{l,z}$, is computed from the equation given below

$$Nu_{l,z} = \frac{T_i^+}{\delta_l^+ T_{av}^+} = \frac{1}{T_{av}^+} \left[-k^+ \frac{\partial T^+}{\partial r^+}\bigg|_{g,i} + \frac{Pr_l}{4S} \frac{\lambda_i^+}{Re_g} \frac{dRe_l}{dz^+} \right] \tag{48}$$

The local convection Nusselt number ($Nu_{g,z}$) and Sherwood number ($Sh_{g,z}$) are computed from the following equations:

$$Nu_{g,z} = -\frac{1}{T^+_{av}}\frac{\partial T^+}{\partial r^+}\bigg|_{g,i} \tag{49}$$

$$Sh_{g,z} = -\frac{1}{\rho^+_{v,av}}\frac{\partial \rho^+_v}{\partial r^+}\bigg|_{i} \tag{50}$$

The average condensate Nusselt number ($Nu_{l,av}$) and Nusselt number ($Nu_{g,av}$) and Sherwood number ($Sh_{g,av}$) of gas phase are computed from their respective local values at each z^+. The average values are obtained as integrated average of local values using Simpson's rule.

$$Nu_{l,av} = \frac{1}{L}\int_0^L Nu_{l,z}\,dz \tag{51}$$

$$Nu_{g,av} = \frac{1}{L}\int_0^L Nu_{g,z}\,dz \tag{52}$$

$$Sh_{g,av} = \frac{1}{L}\int_0^L Sh_{g,z}\,dz \tag{53}$$

2.10. Pressure drop

The total pressure of air–water vapor mixture, P, at any z can be obtained from the following equation:

$$P = \frac{n_T R_u T_{av}}{V} \tag{54}$$

where $n_T = n_v + n_a$, is the total number of moles of air–water vapor mixture and R_u is the universal gas constant. The pressure gradient at any z is given by the following equation:

$$\frac{dP}{dz} = (R_v\rho_v + R_a\rho_a)\frac{dT_{av}}{dz} + R_v T_{av}\frac{d\rho_v}{dz} \tag{55}$$

For z > 0, the vapor density ρ_v decreases with z. The density of vapor ρ_v at the temperature T_{av} is calculated using Eq. (2). Eq. (55) is written as follows:

$$\frac{1}{R_v\rho_{v,0}(T_0 - T_w)}\frac{dP}{dz^+} = \left(\rho^+_v + \frac{R_a\rho_a}{R_v\rho_{v,0}}\right)\frac{dT^+_{av}}{dz^+} + \left(\frac{1}{\beta} + T^+_{av}\right)\frac{d\rho^+_{v,av}}{dz^+} \tag{56}$$

Total pressure drop over the length, L, is calculated as follows:

$$\Delta P = P_0 - P_{z=L}. \tag{57}$$

2.11. Thermo-physical properties

The properties of water vapor are taken at dew point temperature, and the properties of condensate are evaluated at the mean of dew point and wall temperatures. The viscosity, thermal conductivity and specific heat of the vapor–air mixture as functions of those of the vapor and air are calculated making use of the following equations given by Fullarton and Schlunder [36].

$$\mu_g(\text{N s m}^{-2}) = \frac{\left(\sqrt{18}\mu_v Y_v + \sqrt{29}\mu_a Y_a\right)}{\left(\sqrt{18}Y_v + \sqrt{29}Y_a\right)} \tag{58}$$

$$k_g(\text{W m}^{-1}\ \text{K}^{-1}) = \frac{Y_v K_v}{(Y_v + Y_a A)} + \frac{Y_a K_a}{(Y_a + Y_v A)} \tag{59}$$

where

$$A = \frac{1}{3.6}\left[0.8876\left(1 + \sqrt{K_v/K_a}\right)\right]^2$$

$$C_{p,g}(\text{J kg}^{-1}K^{-1}) = Y_v C_{p,v} + Y_a C_{p,a} \tag{60}$$

The diffusion coefficient of water vapor in air, D_{va}, is calculated using the following equation given by Marrero and Mason [37].

$$D_{va}(m^2\ s^{-1}) = \frac{\left(1.87\times10^{-10}\times T^{2.072}\right)}{P} \tag{61}$$

3. Method of solution

The momentum balance equation contains the local pressure gradient, which is unknown. A method is devised to calculate the local pressure gradient at each increment of Δz. An equation for $(\partial P^+/\partial z^+)$ is derived by integrating the normalized momentum balance equation partially with respect to r^+ between the limits 0 to $(0.5 - \delta_l^+)$. The derivative $(\partial u^+/\partial z^+)$ appearing in the normalized momentum balance equation is eliminated making use of the normalized continuity equation. The resulting equation for $(\partial P^+/\partial z^+)$ is given below.

$$\frac{1}{2\rho^+_g}\frac{\partial P^+}{\partial z^+} = \int_0^{0.5}\frac{u^+}{r^+}\frac{\partial(v^+r^+)}{\partial r^+}dr^+ + \frac{1}{\rho^+_g}\frac{\partial \rho^+_g}{\partial z^+}\int_0^{0.5}u^{+2}dr^+ - \int_0^{0.5}v^+\frac{\partial u^+}{\partial r^+}dr^+ + \int_0^{0.5}\frac{1}{r^+}\frac{\partial u^+}{\partial r^+}dr^+ - \frac{\partial u^+}{\partial r^+}\bigg|_{r^+=0.5} + \frac{Ar_0}{2Re_{g,0}} \tag{62}$$

Certain simplifying assumptions are made in Eq. (62) by assuming that $(0.5 - \delta_l^+) = 0.5$ and $Ar/Re_g = Ar_0/Re_{g,0}$, and these assumptions are found to be permissible from the numerical results. The numerical procedure for the solution of the constitutive equations is as follows.

The normalized mass, momentum and energy balance equations and the diffusion equation, i.e., Eqs. (34)–(37) for the gas phase are solved numerically by the implicit finite difference method over the range of interest, viz., $0 \leqslant r^+ \leqslant (0.5 - \delta_l^+)$, $0 \leqslant z^+ \leqslant L^+$. The first derivative of normalized velocity, u^+ in z^+-direction is written in backward difference form (upwind differencing), and that in r^+-direction is written in forward difference form. The higher order derivatives are written in central difference form. The number of grids in r^+-direction is chosen as 200. Oosthuizen and Naylor [38] solved the problem of forced flow in a pipe using an explicit numerical method. They took the value of Δz^+ based on the criterion that $\Delta z^+ \leqslant (\Delta r^{+2}L/DRe_{g,0})$. Since we solved the problem by using an implicit method, we could choose a larger value of Δz^+ than that in an explicit method. However we used the same value of Δz^+as in explicit method, which is given by the inequality given above. The system of equations in finite difference form is cast into a tri-diagonal matrix equation, which is solved by the Thomas algorithm given by Sastry [39]. The values of u^+, T^+ and ρ^+_v are obtained by the following procedure:

(i) The values of P_0, T_0, $R_{H,0}$ and $Re_{g,0}$ at the inlet, i.e., at $z = 0$ are specified. The system parameters are Re_g, Pr_g, Pr_l, S, Sc_g.

(ii) The solution is started at the inlet, i.e., at $z^+ = 0$. An initial guess value is calculated from the following equation for the pressure gradient (dP^+/dz^+) over a distance of Δz^+.

$$\frac{1}{\rho^+_g}\frac{\partial P^+}{\partial z^+} = -\frac{\partial u^+}{\partial r^+}\bigg|_{r^+=0.5} \tag{63}$$

The tri-diagonal matrix obtained from the finite difference analogue of the momentum balance equation i.e., Eq. (35) is solved using Thomas algorithm to get the velocities (u^+) at various values of r^+ at the end of the increment, i.e., at $z^+ = \Delta z^+$. δ_l^+ is computed from Eq. (46) using a procedure which is described later. The assumed value of (dP^+/dz^+) is improved making use of the derived equation, i.e., Eq. (62).

(iii) The momentum balance equation is solved again for the same step of Δz^+ using the improved value of (dP^+/dz^+) to get improved values of u^+ profile at $z^+ = \Delta z^+$. This procedure is repeated until a converged value of (dP^+/dz^+) is obtained over the distance of Δz^+.

(iv) The normalized equations of energy balance and diffusion, i.e., Eqs. (36) and (37) are also numerically solved to obtain

T^+ and ρ_v^+ over an increment of Δz^+ by implicit finite difference method with the aid of Thomas algorithm.

(v) The values of v^+ at all the grid points for $0 \leqslant r^+ \leqslant (0.5 - \delta_l^+)$ are calculated using the normalized equation of continuity, i.e., Eq. (34).

(vi) The converged values of u^+ at the end of the first increment become the inputs for the solution of the momentum balance equation for the next increment in Δz^+. The converged value of (dP^+/dz^+) becomes the initial guess value for the second step of Δz^+. Thus the numerical solution is continued to compute u^+, T^+, ρ_v^+ and v^+ at each increment of Δz^+ until z^+ becomes equal to L^+.

The density gradient $d\rho_g/dz$, at increment Δz^+ is computed as follows. At the inlet of the pipe i.e., at $z = 0$; $T = T_0$ and $\rho_v = \rho_{v,0}$. At each increment in the downstream distance, the average vapor density of the gas phase, $\rho_{v,av}$, is calculated. Making use of the value of $\rho_{v,av}$, the density of the vapor–air mixture, ρ_g is calculated from Eq. (3). The density gradient, $d\rho_g/dz$, is computed from the values of ρ_g over an increment Δz^+. The pressure of the vapor–air mixture at any z is calculated as shown below.

$$p_v = R_v \rho_v T_{av}, \quad p_a = R_a \rho_a T_{av}, \quad P = p_v + p_a. \tag{64}$$

The normalized interface-temperature T_i^+ is calculated by a trail-and-error procedure from Eq. (47) with the aid of Eqs. (43) and (46). A trail value for T_i^+ is assumed, which is used to compute various terms present on RHS of Eq. (47). An approximate value for Re_l is also calculated by integration of Eq. (43) for a step size (Δz^+). Thus the resulting value of RHS of Eq. (47) gives an improved value of T_i^+. The same is used again to compute RHS of Eq. (47). Thus the process of successive approximates is repeated until the evaluated RHS coincides with the assumed T_i^+ within an accuracy of 0.01 percent. The increment in Re_l over step size Δz^+ is obtained from Eq. (43). Thus proceeding with successive step sizes (Δz^+) the value of Re_l at each z^+ (measured from inlet $z = 0$) is known, at any z^+, the $Nu_{l,z}$, $Nu_{g,z}$ and $Sh_{g,z}$ are calculated from Eqs. (48)–(50) respectively. The local pressure is computed making use of Eq. (56). The average values for condensation and convection Nusselt numbers, temperature at the gas-to-liquid interface and Sherwood number are evaluated as integrated averages over the length of the pipe and ΔP_{tot}, the total pressure drop over the length of the pipe is computed making use of Eq. (57). The exit pressure is also obtained during the numerical solution of the momentum balance equation, viz., Eq. (35).

4. Results and discussion

The implicit pressure correction method developed by the authors and given by Eq. (62) is tested for its correctness before using it to solve the current problem. A forced convection heating problem of laminar flow of air in a pipe with constant wall temperature is considered for this purpose. The momentum and energy balance equations are solved by using the implicit pressure correction method. The numerical results for pressure drop and heat transfer coefficient are compared with those calculated from expressions available in literature.

Numerical results are obtained for local values of condensation Nusselt number, $Nu_{l,z}$, condensate Reynolds number, $Re_{l,z}$, and the gas-to-liquid interface temperature, T_i, as functions of normalized downstream distance, z/L, for different values of system parameters. The system parameters considered in the present study are the $R_{H,0}$, the relative humidity of the air at the inlet of the pipe, $Re_{g,0}$, the gas phase Reynolds number at the pipe inlet, T_0, temperature of the air at pipe inlet, and P_0, the total pressure of the air in the pipe at inlet. The average condensation Nusselt number, $Nu_{l,av}$, the condensate Reynolds number at the pipe exit (i.e., at $z = L$), $Re_{l,e}$, average gas-to-liquid interface temperature, $T_{i,av}$, and total pressure drop, ΔP_{tot}, are also computed from numerical results for different values of system parameters. The chosen common parameters are the constant wall temperature, $T_w = 5$ °C, length of the pipe, $L = 1$ m, and the diameter of the pipe, $D = 0.025$ m.

4.1. Effect of system parameters on $Nu_{l,z}$ and $Re_{l,z}$

Fig. 2 shows the effects of the system parameters $R_{H,0}$, $Re_{g,0}$, T_0 and P_0 on the local condensation Nusselt numbers, $Nu_{l,z}$. The heat transfer from humid air during condensation depends on two interdependent effects, viz., sensible heat transfer through the gas film due to the temperature difference between air stream and wall, and the latent heat transfer due to the water vapor mass fraction difference. At prescribed values of P_0, T_0 and $Re_{g,0}$, with decrease in $R_{H,0}$ the water vapor content of the mixture at inlet decreases. The latent heat transfer and consequently the total heat transfer to the condensate film decreases with decrease in $R_{H,0}$. Therefore, the local condensation Nusselt numbers decrease with a decrease in $R_{H,0}$. The same trend can be observed from the curves 1 and 2 of Fig. 2. The curves 2 and 3 of Fig. 2 show the variation of local condensation Nusselt number, $Nu_{l,z}$ with inlet temperature of air, T_0. At a given system pressure, P_0, relative humidity, $R_{H,0}$, and mixture Reynolds number, $Re_{g,0}$, the latent heat transfer to the liquid film increases with an increase in T_0 due to increase in the saturation vapor pressure and a resulting increase in the vapor density. The heat transfer by convection also increases due to an increase in the temperature difference between the gas–vapor mixture core and wall with an increase in T_0. Hence $Nu_{l,z}$ increases with the increase in T_0 due to increase in total heat transfer to the condensate film. The curves 2 and 4 of Fig. 2 show the effect of $Re_{g,0}$ on $Nu_{l,z}$ when the other system parameters remain the same. At a constant value $R_{H,0}$ an increase in the gas phase Reynolds number at inlet ($Re_{g,0}$) results in an increase in the flow rate of the vapor. Hence the local condensation Nusselt numbers increases with an increase in $Re_{g,0}$. The curves 2, 5 and 6 of Fig. 2 show the effect of P_0, the pressure of humid air at the inlet on the $Nu_{l,z}$. As P_0, decreases the density and saturation temperature of the vapor–gas mixture decrease facilitating easier condensation of the vapor for a prescribed set of system parameters, namely $R_{H,0}$, T_0, and $Re_{g,0}$. Thus the curves 2, 5 and 6 indicate an increase in $Nu_{l,z}$ with a

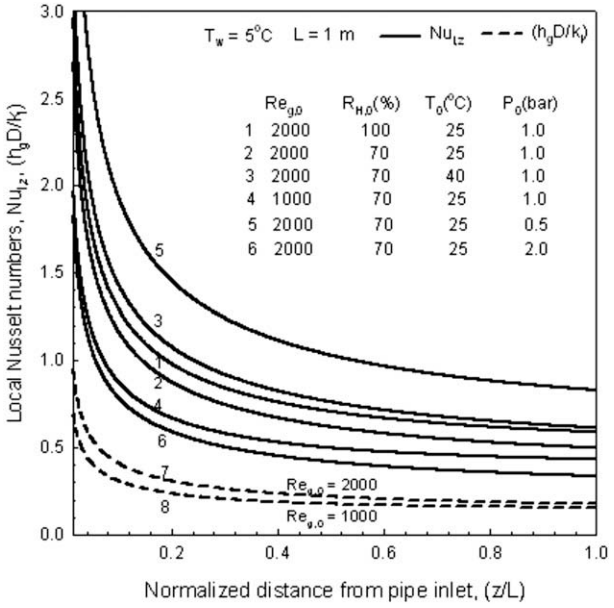

Fig. 2. Effect of T_0, $Re_{g,0}$, P_0 and $R_{H,0}$ on local Nusselt numbers.

decrease in P_0. The gas phase Nusselt number (h_gD/k_l), which represents the convection part of the total heat transfer, is shown plotted by the dashed line in Fig. 2 for two different values of $Re_{g,0}$. The curves 7 ($Re_{g,0}$ = 2000) and 8 ($Re_{g,0}$ = 1000) of Fig. 2 show that the gas phase Nusselt number (h_gD/k_l) increases with an increase in $Re_{g,0}$. However the effects of $R_{H,0}$, T_0 and P_0 on gas phase Nusselt number ($Nu_{g,z}$) are not significant.

Fig. 3 shows the effects of the system parameters $R_{H,0}$, $Re_{g,0}$, T_0 and P_0 on the local condensate Reynolds number, $Re_{l,z}$ as a function of the downstream distance, (z/L). As explained previously an increase in $R_{H,0}$ (curves 1 and 2), T_0 (curves 2 and 3), and $Re_{g,0}$ (curves 2 and 4) the local condensate Reynolds number, $Re_{l,z}$, increases due to increase in vapor density of the mixture towards the condensation surface. The $Re_{l,z}$ increases with a decrease in total pressure at inlet, P_0 (curves 2, 5 and 6) due to decrease in saturation temperature and the resulting decrease in density of mixture.

4.2. Effect of $R_{H,0}$, $Re_{g,0}$, T_0 and P_0 on local gas-to-liquid interface temperature (T_i)

The effects of the system parameters $R_{H,0}$, $Re_{g,0}$, T_0 and P_0 on the local gas–liquid interface temperature, T_i are shown plotted Fig. 4. The curves 1 and 2 of Fig. 4 show increase in T_i with an increase in $R_{H,0}$. The latent heat transferred to the condensate film increases with an increase in $R_{H,0}$ for a given $Re_{g,0}$, T_0 and P_0, due to increase in water content of air with an increase in $R_{H,0}$. At fixed values of $R_{H,0}$, $Re_{g,0}$, and P_0 the gas–liquid interface temperature, T_i, increases with T_0, which can be attributed to the increase in latent and convection heat transfers to the condensate film due to an increase in dew point temperature of the mixture and difference between mixture core and wall temperatures respectively. The same can be observed from curves 2 and 3 of Fig. 4. The curves 2, 5 and 6 of the same figure show the variation of $T_i$with P_0 at fixed $R_{H,0}$, $Re_{g,0}$, T_0. The heat transfer to the condensate film increases due to a decrease in saturation temperature of mixture with decrease in P_0, and hence the T_i increases with a decrease in P_0. The variation in magnitude of T_i with $Re_{g,0}$is not significant, since the variation of magnitude of $Re_{g,0}$ in laminar flow is not high. The curves 2 and 4 of Fig. 4 indicate a marginal change in T_i with an increase in $Re_{g,0}$.

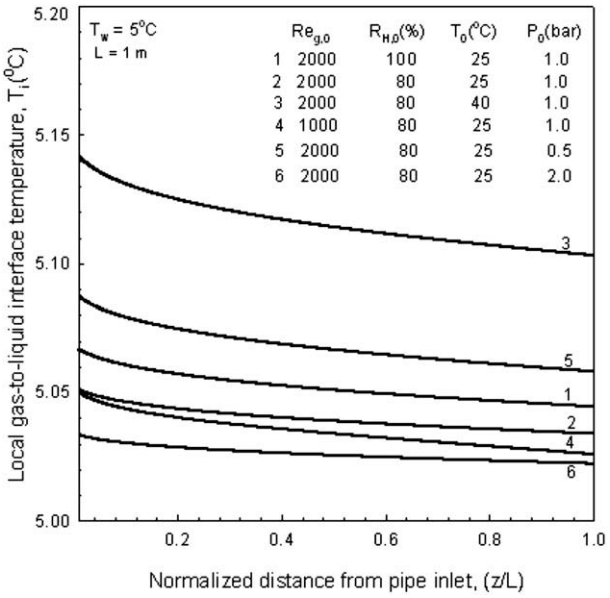

Fig. 4. Effect of T_0, P_0, $Re_{g,0}$ and $R_{H,0}$ on gas-to-liquid interface temperature.

4.3. Effect of $Re_{g,0}$ and T_0 on local vapor–gas mixture temperature (T_z)

The effect of $Re_{g,0}$ on local vapor–gas mixture temperature, T_z, for two different inlet temperatures of air, viz., T_0 = 25 °C and T_0 = 40 °C is shown plotted in Fig. 5 as a function of normalized downstream distance, z/L. The temperature of the gas–vapor mixture decreases along the length of the pipe due to latent and convection heat transfer from the vapor–gas mixture to the cold wall. The latent heat is released due to condensation of vapor and the heat released by convection is due to temperature difference between the vapor–gas mixture and cold wall. A decrease in T_z is observed with a decrease in $Re_{g,0}$ for prescribed value T_0, which may be attributed to the increase in the residential time of vapor–gas mixture in the pipe.

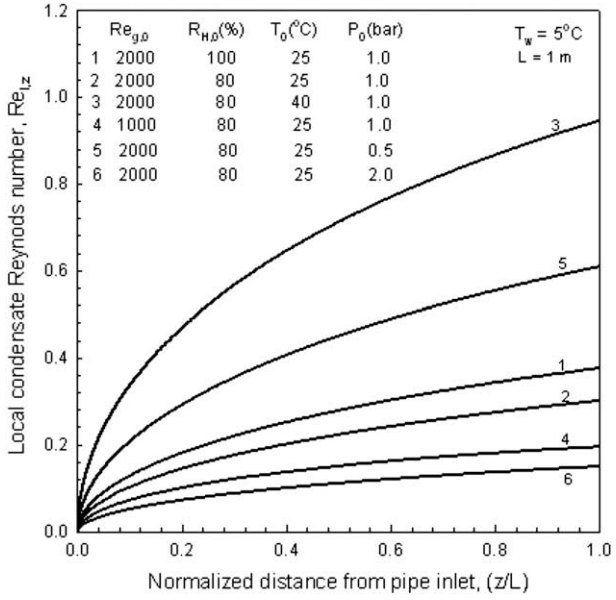

Fig. 3. Variation of $Re_{l,z}$ with T_0, $Re_{g,0}$, P_0 and $R_{H,0}$.

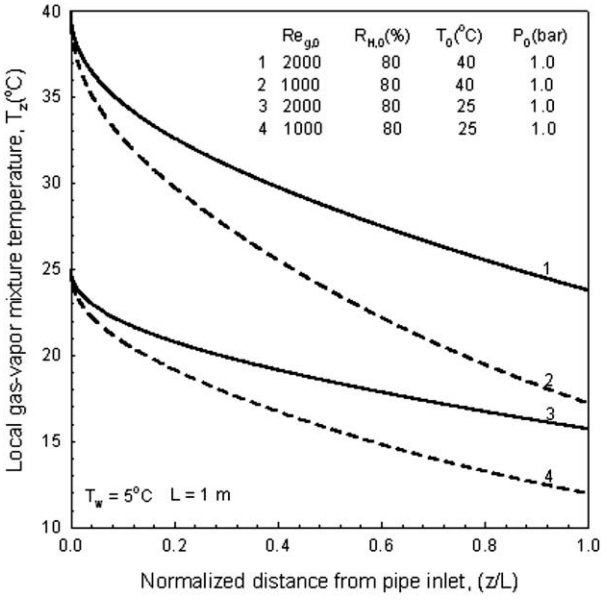

Fig. 5. Variation of local gas–vapor mixture temperature (T_z) with T_0 and $Re_{g,0}$.

4.4. Effect of $R_{H,0}$ and T_0 on $Nu_{l,av}$, $Re_{l,e}$, $T_{i,av}$ and ΔP_{tot}

Fig. 6 shows the variation of average condensation Nusselt number, $Nu_{l,av}$ and the condensate Reynolds number at the pipe exit (i.e., at $z = L$), $Re_{l,e}$ with $R_{H,0}$, ranging from 50 to 100% for two different values of T_0 ($T_0 = 25$ °C and $T_0 = 40$°C) for constant values of $Re_{g,0} = 2000$ and $P_0 = 1$ bar. The $Nu_{l,av}$ lies between 0.574 to 0.902 for $T_0 = 25$ °C (curve 1) and lies between 0.69 and 1.138 for $T_0 = 40$ °C (curve 2). The $Nu_{l,av}$ increases due to increase in latent heat transfer with an increase $R_{H,0}$, and an increase in latent as well as sensible heat transfer with increase in T_0. The $Re_{l,e}$ varies from 0.188 to 0.3764 for $T_0 = 25$ °C (curve 3) and lies between 0.5896 and 1.1825 for $T_0 = 40$ °C (curve 4). As discussed earlier, the $Re_{l,e}$ increases with an increase in $R_{H,0}$ and T_0 due to increase in the rate of condensation of water vapor towards the wall.

The effects of relative humidity ($R_{H,0}$) and air temperature (T_0) at the inlet on the variation of $T_{i,av}$, the average gas-to-liquid interface temperature and ΔP_{tot}, total pressure drop are shown in Fig. 7. The common parameters chosen are $Re_{g,0} = 2000$ and $P_0 = 1$ bar. Numerical results are obtained for the same range of $R_{H,0}$ and same values of T_0 i.e.,$T_0 = 25$ °C and $T_0 = 40$ °C. The $T_{i,av}$ lies between 5.023 °C and 5.052 °C (curve 1) at $T_0 = 25$ °C and lies between 5.066 °C and 5.155 °C (curve2) at $T_0 = 40$ °C. The $T_{i,av}$ increases very marginally with an increase in $R_{H,0}$ and T_0, due to the increase in total heat transfer to the condensate film. The two-phase pressure drop is also an important phenomenon in in-tube condensation. The curves 3 and 4 of Fig. 7 indicate that ΔP_{tot} varies from 3.883 kPa to 4.638 kPa for $T_0 = 25$ °C and varies from 6.944 kPa to 8.659 kPa for $T_0 = 40$ °C, respectively. The partial pressure of water vapor in the water vapor–air mixture increases with an increase in the value of $R_{H,0}$, and with increase in the gas inlet temperature (T_0) the saturation vapor pressure increases. Hence the ΔP_{tot} increases with an increase in $R_{H,0}$ and T_0. It is also observed that the frictional component of the pressure drop ΔP_{fr}, is considerably a low fraction of the total pressure drop, ΔP_{tot} and remains almost constant at different values of $R_{H,0}$, but varies slightly when T_0 is changed.

4.5. Effect of $Re_{g,0}$ on $Nu_{l,av}$, $Re_{l,e}$, $Nu_{g,av}$ and $Sh_{g,av}$

Fig. 8 shows the variation of $Nu_{l,av}$, $Re_{l,e}$ and average gas phase Nusselt ($Nu_{g,av} \times k^+$) and Sherwood numbers ($Sh_{g,av} \times k^+$) with

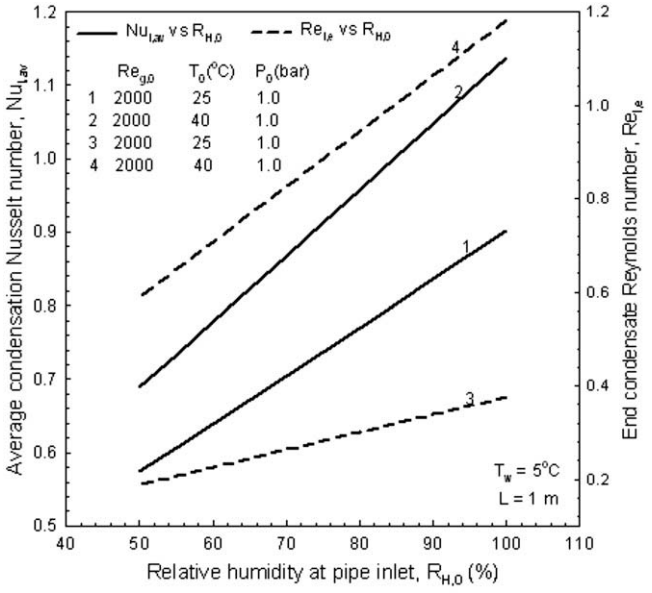

Fig. 6. Effect of relative humidity at pipe inlet on $Nu_{l,av}$ and $Re_{l,e}$.

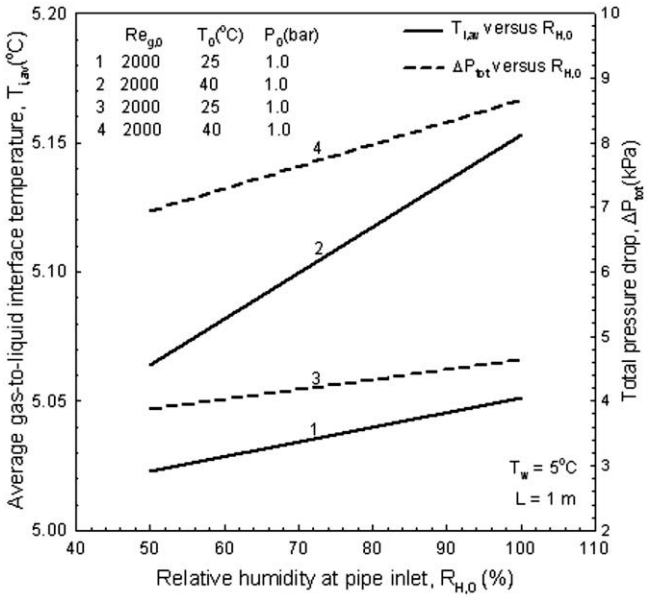

Fig. 7. Effect of relative humidity at pipe inlet on $T_{i,av}$ and ΔP_{tot}.

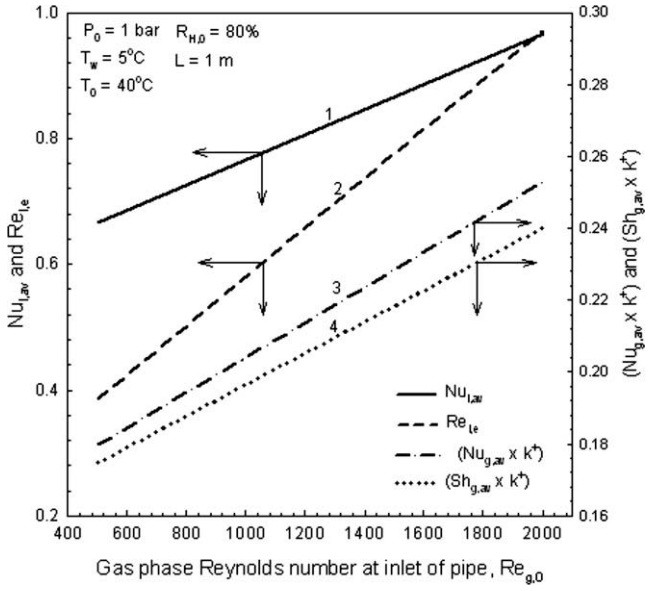

Fig. 8. Effect of $Re_{g,0}$ on $Nu_{l,av}$, $Re_{l,e}$, $Nu_{g,av}$ and $Sh_{g,av}$.

$Re_{g,0}$, ranging from 500 to 2000. The common parameters chosen are $P_0 = 1$ bar, $R_{H,0} = 80\%$, $T_w = 5$ °C and $T_0 = 40$ °C. The $Nu_{l,av}$ lies between 0.6545 and 0.9577 (curve 1) and $Re_{l,e}$ varies from 0.3493 to 0.945 (curve 2). As expected, the $Nu_{l,av}$, $Re_{l,e}$ increases with an increase in $Re_{g,0}$ due to increase in the flow rate of vapor. The average gas phase Nusselt and Sherwood numbers are also calculated for different values of $Re_{g,0}$and are shown in the same figure as curves 3 and 4, respectively. The Nusselt and Sherwood numbers are close enough to one other, since the Prandtl and Schmidt numbers are nearly the same for air.

4.6. Effect of $Re_{g,0}$ and T_0 on $T_{i,av}$ and ΔP_{tot}

The effect of $Re_{g,0}$ on $T_{i,av}$ and ΔP_{tot} is shown in Fig. 9 for prescribed values of $P_0 = 1$ bar and $R_{H,0} = 80\%$. The $T_{i,av}$ increases from 5.027 °C to 5.04 °C for T_0= 25 °C (see curve 1) and varies from 5.084 °C to 5.116 °C for $T_0 = 40$ °C (see curve 2) as $Re_{g,0}$ increases

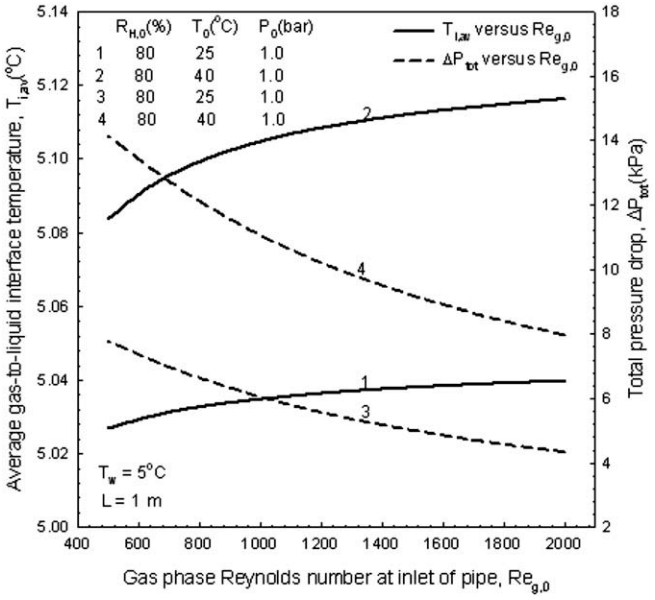

Fig. 9. Variation of $T_{i,av}$ and ΔP_{tot} with $Re_{g,0}$.

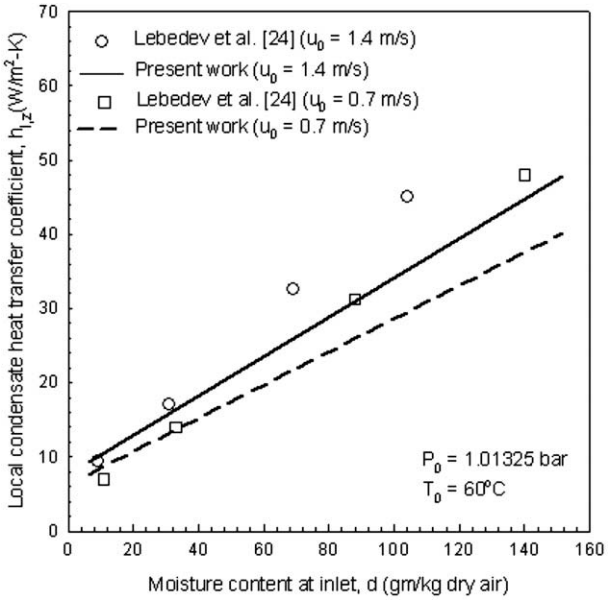

Fig. 11. Comparison of $h_{l,z}$ of present work with experimental data of Lebedev et al. [24].

from 500 to 2000 due to an increase in heat transfer to the condensate film. The curves 3 and 4 of Fig. 9 show that the ΔP_{tot} decreases with an increase in $Re_{g,0}$. The lesser pressure drop at a higher $Re_{g,0}$ is due to the smaller change in the mass flow rate of the gas–vapor mixture from inlet to exit at a higher value of $Re_{g,0}$. However, the frictional component of pressure drop, ΔP_{fr}, increases as $Re_{g,0}$ increases from 500 to 2000.

4.7. Effect of P_0 on $Nu_{l,av}$, $Re_{l,e}$ and $T_{i,av}$

Fig. 10 shows the variation of $Nu_{l,av}$, the average condensation Nusselt number, $Re_{l,e}$, the condensate Reynolds number at the pipe exit, and $T_{i,av}$, the average gas-to-liquid interface temperature with P_0, ranging from 0.5 to 2.5 bar. The chosen common parameters are $T_0 = 25$ °C, $Re_{g,0} = 1500$, $R_{H,0} = 70\%$. The $Nu_{l,av}$ decreases from 1.1938 to 0.4378, $Re_{l,e}$ changes from 0.54765 to 0.1081 and $T_{i,av}$ decreases from 5.068 to 5.025 as the total pressure at inlet increases from 0.5 to 2.5 bar due to the high rate of condensation at lower system pressures.

4.8. Comparison with experimental data

To the best of our knowledge, there are no experimental results available in literature for the geometry of the pipe, viz., for the case of condensation of vapor from a mixture of vapor and high-concentration non-condensable gas in laminar flow through a vertical tube. So the present theoretical work is compared with the experimental data of Lebedev et al. [24], who conducted experiments in a vertical duct to study the heat and mass transfer in the condensation of vapor from humid air in a pre-turbulent flow. The exper-

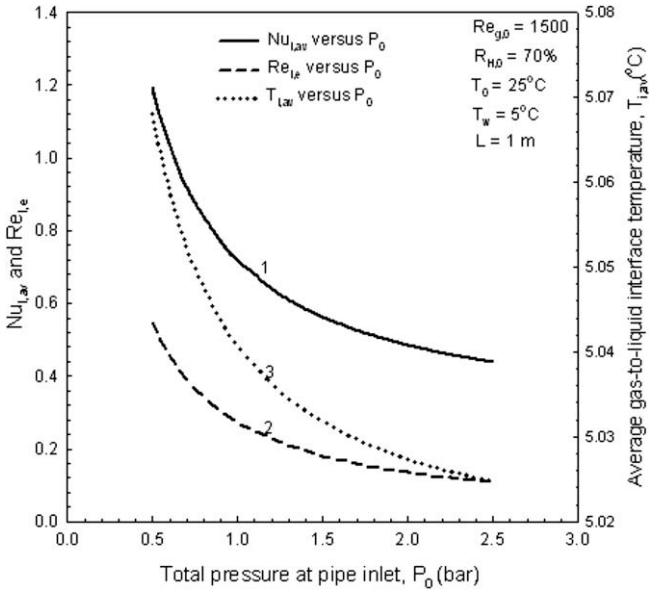

Fig. 10. Effect of total pressure at pipe inlet on $Nu_{l,av}$, $Re_{l,e}$ and $T_{i,av}$.

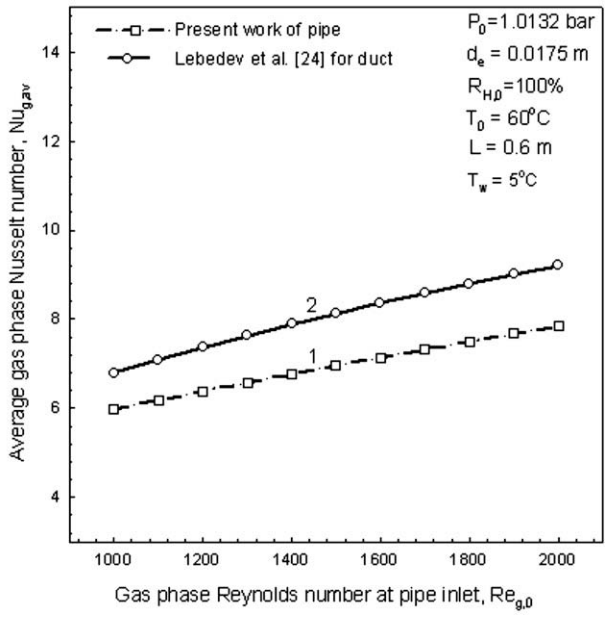

Fig. 12. Comparison of $Nu_{g,av}$ of present work with Lebedev et al. [24].

imental set up of Lebedev et al. [24] consists of a rectangular duct 0.02 m wide, 0.15 m high and 0.6 m long. They obtained experimental data for condensation heat transfer coefficients at two different velocities at inlet, viz., $u_0 = 1.4$ m/s ($Re_{g,0} = 1480$) and $u_0 = 0.7$ m/s ($Re_{g,0} = 740$), which are shown in Fig. 11. Numerical results are obtained for the same conditions of gas Reynolds number ($Re_{g,0}$), gas inlet temperature (T_0) and total pressure of gas–vapor mixture at inlet (P_0)as those of Lebedev et al. [24]. The other data used are as follows, $R_{H,0} = 100\%$, $P_0 = 1.01325$ bar, $L = 0.6$ m and $d_e = 0.02$ m, where d_e is the equivalent diameter for the case of duct. The condensation heat transfer coefficients computed at the middle of test section are shown in Fig. 11, which show satisfactory agreement with the experimental data of Lebedev et al. [24]. Lebedev et al. [24] also developed a correlation for average gas phase Nusselt number from the experimental results. It can be observed from curves 1 and 2 of Fig. 12 that the average gas phase Nusselt numbers, $Nu_{g,av}$, computed from the present theory (curve 1) are close enough to the experimental data (curve 2) of Lebedev et al. [24] for chosen common parameters of $T_0 = 60$ °C and $Re_{g,0}$ ranging from 1000 to 2000. The other data used are as follows, $R_{H,0} = 100\%$, $P_0 = 1.01325$ bar, $T_w = 5$ °C, $L = 0.6$ m and $d_e = 0.0175$ m.

5. Conclusions

1. A theoretical model is developed for the case of in-tube laminar film condensation of water vapor in the presence of high concentration non-condensable gas, when the gas–vapor mixture flows inside a vertical tube under laminar forced flow conditions.
2. The salient system parameters controlling the process are found to be T_0, $Re_{g,0}$, $R_{H,0}$ and P_0. Numerical results are obtained for wide range of the system parameters.
3. From the numerical results the local and average Nusselt numbers, condensate Reynolds number, gas–liquid interface temperature and pressure drop are estimated. The variation of local gas–vapor mixture temperature along the length of the pipe is also estimated.
4. The condensation heat transfer coefficients and the rate of condensation decreases considerably in the presence of non-condensable gas in high percentage.
5. The numerical results of the present theoretical study agree satisfactorily with the experimental data available in literature.
6. An example of water vapor–air mixture is considered in view of its wide practical utility. However this theoretical model can be applied to any vapor–gas combination with suitable substitution of property values.

References

[1] E.F. Carpenter, A.P. Colburn, The effect of vapor velocity on condensation inside tubes, in: Proceedings of the General Discussion on Heat Transfer, IMechE/ASME, 1951, pp. 20–26.
[2] I. Shekriladze, S.H. Mestvirishvili, High-rate condensation process theory of vapor flow inside a vertical cylinder, Int. J. Heat Mass Transfer 16 (1973) 715–724.
[3] K. Lucas, B. Moser, Laminar film condensation of pure vapors in tubes, Int. J. Heat Mass Transfer 22 (1979) 431–435.
[4] F. Dobran, R.S. Thorsen, Forced flow laminar film wise condensation of a pure saturated vapor in a vertical tube, Int. J. Heat Mass Transfer 23 (1980) 161–177.
[5] R.A. Seban, J.A. Hodgson, Laminar film condensation in a tube with upward vapor flow, Int. J. Heat Mass Transfer 25 (1982) 1291–1300.
[6] F. Blangetti, R. Krebs, E.U. Schlunder, Condensation in vertical tubes – experimental results and modeling, Chem. Eng. Fund. 1 (2) (1982) 20–42.
[7] S.J. Kim, H.C. No, Turbulent film condensation of high pressure steam in a vertical tube, Int. J. Heat Mass Transfer 43 (2000) 4031–4042.
[8] V.M. Borishansky, D.I. Volkov, N.I. Ivashchenko, Effects of non-condensable gas content on heat transfer in steam condensation in a vertical tube, Heat Transfer Sov. Res. 9 (2) (1977) 35–42.
[9] C.Y. Wang, C.J. Tu, Effects of non-condensable gas on laminar film condensation in a vertical tube, Int. J. Heat Mass Transfer 31 (1988) 2339–2345.
[10] T. Kageyama, P.F. Peterson, V.E. Schrock, Diffusion layer modeling for condensation in vertical tubes with non-condensable gases, Nucl. Eng. Des. 141 (1993) 289–302.
[11] P.F. Peterson, V.E. Schrock, T. Kageyama, Diffusion layer theory for turbulent vapor condensation with non-condensable gases, ASME J. Heat Transfer 115 (1993) 998–1003.
[12] M. Siddique, M.W. Golay, M.S. Kazimi, Local heat transfer coefficients for forced-convection condensation of steam in a vertical tube in the presence of a non-condensable gas, Nucl. Technol. 102 (1993) 386–402.
[13] M. Siddique, M.W. Golay, M.S. Kazimi, Theoretical modeling of forced convection condensation of steam in a vertical tube in the presence of a non-condensable gas, Nucl. Technol. 106 (1994) 202–214.
[14] H.A. Hasanein, M.S. Kazimi, M.W. Golay, Forced convection in-tube steam condensation in the presence of non-condensable gases, Int. J. Heat Mass Transfer 39 (1996) 2625–2639.
[15] J.L. Munoz-Cobo, L. Herranz, J. Sancho, I. Tkachenko, G. Verdu, Turbulent vapor condensation with non-condensable gases in vertical tubes, Int. J. Heat Mass Transfer 39 (1996) 3249–3260.
[16] A. Dehbi, S. Guentay, A model for performance of a vertical tube condenser in the presence of non-condensable gases, Nucl. Eng. Des. 177 (1997) 41–52.
[17] S.Z. Kuhn, V.E. Schrock, P.F. Peterson, An investigation of condensation from steam–gas mixtures flowing downward inside a vertical tube, Nucl. Eng. Des. 177 (1997) 53–69.
[18] L.E. Herranz, J.L. Munoz-Cobo, G. Verdu, Heat transfer modeling in the vertical tubes of the passive containment cooling system of the simplified boiling water reactor, Nucl. Eng. Des. 178 (1997) 29–44.
[19] H.C. No, H.S. Park, Non-iterative condensation modeling for steam condensation with non-condensable gas in a vertical tube, Int. J. Heat Mass Transfer 45 (2002) 845–854.
[20] N.K. Maheshwari, D. Saha, R.K. Sinha, M. Aritomi, Investigation on condensation in presence of a non-condensable gas for a wide range of Reynolds number, Nucl. Eng. Des. 227 (2004) 219–238.
[21] S. Oh, S.T. Revankar, Experimental and theoretical investigation of film condensation with non-condensable gas, Int. J. Heat Mass Transfer 49 (2006) 2523–2534.
[22] E.C. Siow, S.J. Ormiston, H.M. Soliman, A two-phase model for laminar film condensation from steam–air mixtures in vertical parallel-plate channels, Heat Mass Transfer 40 (2004) 365–375.
[23] M.K. Groff, S.J. Ormiston, H.M. Soliman, Numerical solution of film condensation from turbulent flow of vapor–gas mixtures in vertical tubes, Int. J. Heat Mass Transfer 50 (2007) 3899–3912.
[24] P.D. Lebedev, A.M. Baklastov, Zh.F. Sergazin, Aerodynamics, heat and mass transfer in vapor condensation from humid air on a flat plate in a longitudinal flow in asymmetrically cooled slot, Int. J. Heat Mass Transfer 12 (1969) 833–841.
[25] B.M. Smol'skii, P.A. Novikov, L.A. Shcherbakov, Heat and mass transfer during condensation of water vapor from moist air in narrow channels, IFZh 21 (1971) 71–74.
[26] P.A. Novikov, L.A. Shcherbakov, Heat and mass transfer during droplet condensation of water vapor from a stream of rarefied humid air in narrow rectangular channels, IFZh 23 (1972) 737–742.
[27] B.M. Smol'skii, P.A. Novikov, L.A. Shcherbakov, The mechanism of vapor condensation from humid air in narrow channels and the hydrodynamics of a two-phase flow during droplet condensation, IFZh 24 (1973) 240–244.
[28] G. Desrayaud, G. Lauriat, Heat and mass transfer analogy for condensation of humid air in a vertical channel, Heat Mass Transfer 37 (2001) 67–76.
[29] C. Pele, B. Baudoin, J.P. Barrand, Effect of humid air flow rate on the film-wise condensation inside a vertical cooled pipe: numerical and experimental study, Int. J. Heat Mass Transfer 37 (1994) 1829–1837.
[30] V.I. Terekhov, V.V. Terekhov, K.A. Sharov, Heat and mass transfer during steam condensation from humid air, IFZh 71 (1998) 788–794.
[31] V.I. Terekhov, V.N. Patrikeev, Forced convection heat and mass transfer from pressurized humid air in the channel, Rus. J. Eng. Thermo-phys. 9 (1–2) (1999) 1–18.
[32] E.P. Volchkov, V.V. Terekhov, V.I. Terekhov, A numerical study of boundary-layer heat and mass transfer in a forced flow of humid air with surface steam condensation, Int. J. Heat Mass Transfer 47 (2004) 1473–1481.
[33] V. Dharma Rao, V. Murali Krishna, K.V. Sharma, P.K. Sarma, A theoretical study on convective condensation of water vapor from humid air in turbulent flow in a vertical duct, ASME J. Heat Transfer 129 (2007) 1627–1637.
[34] Ernst Schmidt (prepared), Ulrich Grigull (edited), Properties of Water and Steam in SI units, Springer-Verlag, New York, 1982.
[35] Kenneth Wark Jr., Donald E. Richards, Thermodynamics, sixth ed., WCB-McGraw-Hill, New York, 1999. pp. 651–652.
[36] D. Fullarton, E.U. Schlunder, Approximate calculation of heat exchanger area for condensation of gas–vapor mixtures, Int. Chem. Eng. 26 (3) (1986) 408–418.
[37] T.R. Marrero, E.A. Mason, Gaseous diffusion coefficients, J. Phys. Chem. Ref. Data 1 (1972) 3–118.
[38] P.H. Oosthuizen, D. Naylor, Introduction to Convective Heat Transfer Analysis, McGraw-Hill, New York, 1999. pp. 209–210.
[39] S.S. Sastry, Introductory Methods of Numerical Analysis, fourth ed., Prentice Hall of India Private Limited, New Delhi, 2006. pp. 270–271.